

# Linear Proportional Control of Flow Over a Sphere

**Seung Jeon and Haecheon Choi\***

*School of Mechanical and Aerospace Engineering, Seoul National University, Korea*

*Corresponding author: choi@snu.ac.kr*

**Abstract.** In the present study, we apply a linear proportional control to flow over a sphere for reduction of drag and lift fluctuations. For this purpose, we measure the radial velocity along the centerline in the wake and provide blowing and suction at a part of sphere surface based on the measured velocity. Zero-net mass flow rate is satisfied during the control. This control is applied to the flow over a sphere at  $Re=300$  and  $425$ . We vary the sensing location at  $0.8d \leq x_s \leq 1.3d$  and find that the most effective sensing region coincides with the location at which negative maximum correlation between the lift and sensing-velocity directions occurs. As a result, the lift and drag fluctuations are significantly reduced.

**Key words:** drag, lift, sphere, linear proportional control.

## 1. Introduction

The vortex shedding behind a bluff body produces the drag and lift fluctuations, and thus it is important to reduce these fluctuations in practical situations by introducing some control actions. Therefore, many control methods have been suggested to weaken or annihilate vortex shedding behind a bluff body. However, most methods presented so far are for two-dimensional bodies and control methods for three-dimensional bodies are still limited [4].

The sphere is a representative shape of three-dimensional bluff bodies. Although the sphere is a simple geometry, the vortex shedding behind it is completely three-dimensional and complex. Because of these three-dimensionality and complexity, the control of this flow is not an easy task. Therefore, only a few studies for control of flow over a sphere have been suggested so far: for example, roughness by Achenbach [1], dimples by Bearman and Harvey [3] and Choi *et al.* [5], high-frequency forcing by Kim and Durbin [8], ventilation by Suryanarayana *et al.* [12], high-frequency forcing by Jeon *et al.* [6]. Although these methods are quite effective, they are valid only for subcritical Reynolds numbers.

In the present study, we focus on the flow over a sphere at low Reynolds numbers and apply a linear proportional control to this flow to see if it can reduce the lift and drag fluctuations. Our linear proportional control is based on that proposed by Park *et al.* [11] applied for the control of flow over a two-dimensional circular cylinder. In that study, they successfully suppressed two-dimensional vortex shedding at low Reynolds numbers. Therefore, it should be

interesting to investigate the applicability of this control method to three-dimensional vortex shedding like the flow considered in the present study.

## 2. Numerical details

An immersed boundary method [9] is used to simulate flow over a sphere. The governing equation is the incompressible Navier-Stokes and continuity equations with the immersed boundary method in the cylindrical coordinates:

$$\frac{\partial u_i}{\partial t} + \frac{\partial u_i u_j}{\partial x_j} = -\frac{\partial p}{\partial x_i} + \frac{1}{\text{Re}} \frac{\partial^2 u_i}{\partial x_j \partial x_j} + f_i, \quad (1)$$

$$\frac{\partial u_i}{\partial x_i} - q = 0, \quad (2)$$

where  $t$  is time,  $x_i$  are the cylindrical coordinates,  $u_i$  are the corresponding velocity components,  $p$  is the pressure and  $\text{Re} = U_\infty d / \nu$  is the Reynolds number. Here  $U_\infty$  is the free-stream velocity,  $d$  is the sphere diameter, and  $\nu$  is the kinematic viscosity.  $f_i$  are the momentum forcing and  $q$  is the mass source/sink proposed by Kim *et al.* [9]

To solve these equations, we use the fractional step method [10]. A semi-implicit method proposed by Akselvoll and Moin [2] is used for the time integration. A Dirichlet boundary condition ( $u_x = 1$ ,  $u_r = 0$ ,  $u_\theta = 0$ ) is used for inflow and far-field boundaries and a convective boundary condition ( $\partial u_i / \partial t + c \partial u_i / \partial x = 0$ , where  $c$  is the space-averaged streamwise velocity at the exit) is used for the outflow boundary condition. The size of computational domain is  $-15d \leq x \leq 15d$ ,  $0 \leq r \leq 15d$  and  $0 \leq \theta < 2\pi$ . We simulate the flow at two different Reynolds numbers ( $\text{Re}=300$  and  $425$ ). Without control, the vortical structures behind the sphere are unsteady planar symmetric at  $\text{Re}=300$  and unsteady asymmetric at  $\text{Re}=425$ , respectively. The numbers of grid points are  $289(x) \times 161(r) \times 65(\theta)$  and  $449(x) \times 161(r) \times 65(\theta)$ , respectively, for  $\text{Re}=300$  and  $425$ .

## 3. Linear proportional control

We apply a linear proportional control similar to that proposed by Park *et al.* [11]. The velocity at the centerline in the wake region is measured for feedback and the control input (blowing/suction) at a part of the sphere surface is determined by the measured velocity as follows (Figure 1):

$$\psi(\theta) = \alpha |u_{r,\text{sensed}}| \cos(\theta - \theta'). \quad (3)$$

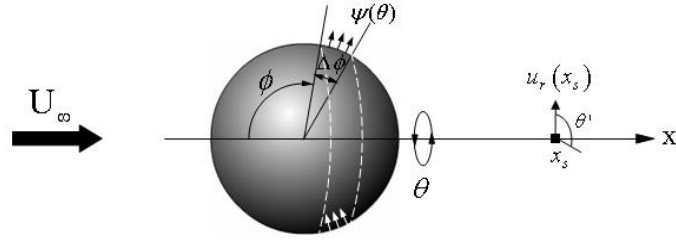


Figure 1. Schematic diagram of the linear proportional control.

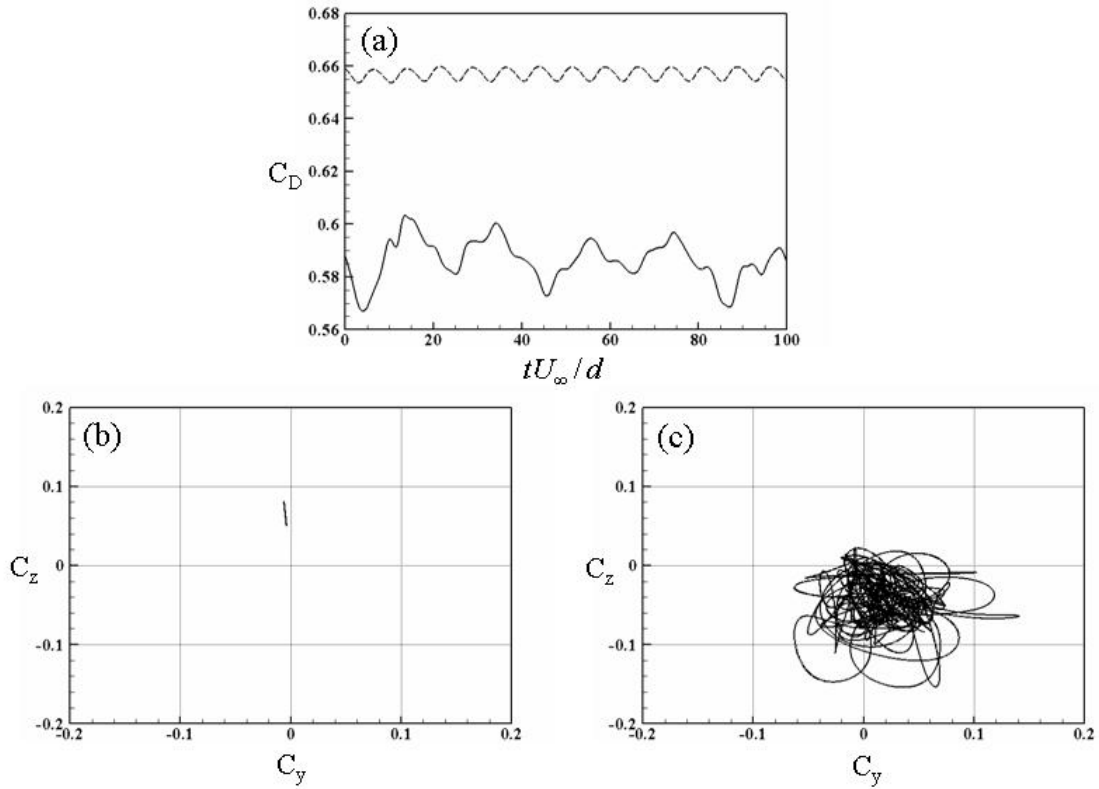


Figure 2. Time histories of the drag coefficient and phase diagram of the lift coefficient (without control): ---,  $Re=300$ ; —,  $Re=425$ . (a) Time histories of drag coefficient; (b) phase diagram of the lift coefficient at  $Re=300$ ; (c) phase diagram of the lift coefficient at  $Re=425$ .

Here,  $\psi$  is the wall-normal actuation velocity (blowing/suction),  $\theta$  is the azimuthal angle,  $\alpha$  is the feedback gain,  $|u_{r,sensed}|$  is the magnitude of measured velocity at the sensing position,  $x_s$ , and  $\theta'$  is the azimuthal angle of measured velocity. Thus, the blowing/suction varies along the azimuthal direction and maximum blowing and suction occur in phase and out of phase to the measured velocity at  $x_s$ . Also the amplitude of blowing/suction linearly increases as the

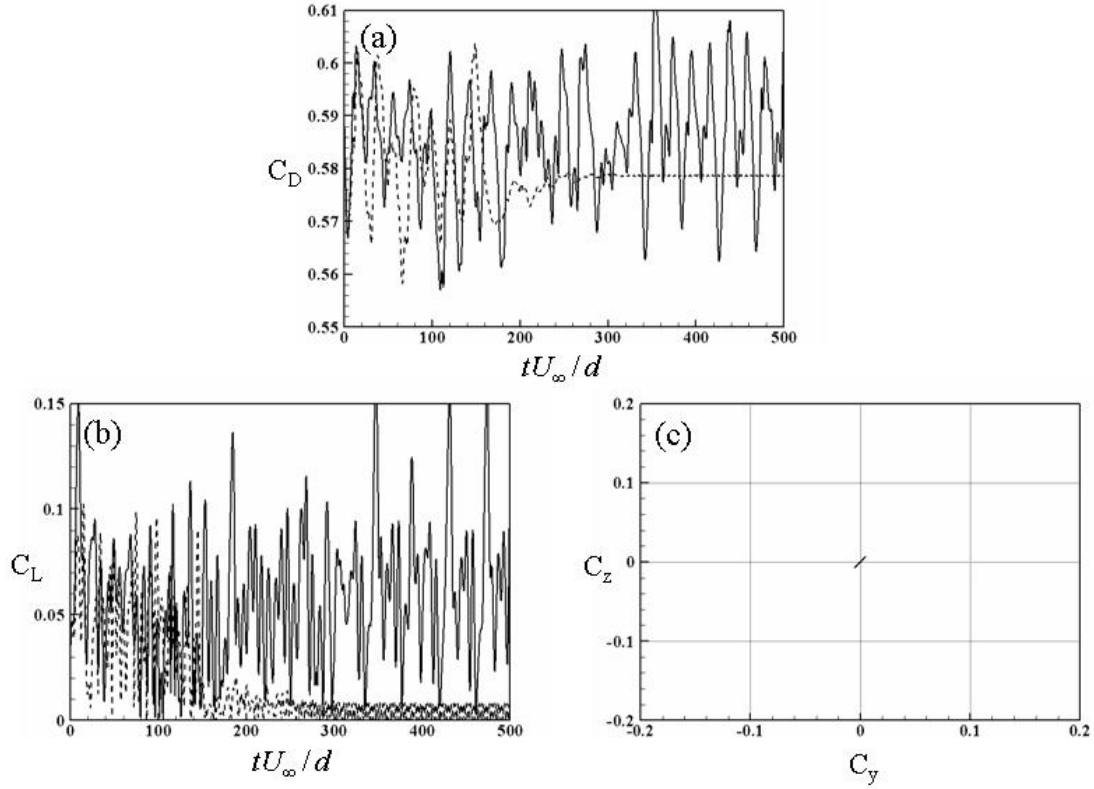


Figure 3. Time histories of the drag and lift coefficients and phase diagram ( $Re=425$ ): (a) time histories of drag coefficient; (b) time histories of the lift coefficient; (c) phase diagram of the lift fluctuations. —, Without control; ---, with control. Shown here is the case of  $x_s = 1.2d$  and  $\alpha = -0.5$ .

measured velocity increases. Various sensing positions are tested. For the actuation location, we set  $\phi = 100^\circ$  and  $\Delta\phi = 20^\circ$  (see Figure 1).

#### 4. Results

The laminar flow over a sphere has four different flow regimes. The vortical structures in the wake are steady axisymmetric, steady planar symmetric, unsteady planar symmetric and unsteady asymmetric as the Reynolds number increases. We consider the cases of  $Re=300$  and  $425$ , at which the flows are unsteady planar symmetric and unsteady asymmetric, respectively. The results of base-flow simulations agree well with those of the previous study [7]. Figure 2 shows the drag and lift coefficients without control. As shown in Figure 2, the drag and lift fluctuations at  $Re=425$  are much larger than those at  $Re=300$ . Thus, we focus on the case of  $Re=425$  mainly in this study.

For the feedback, we choose the sensing position ( $x_s$ ) and amplification coefficient ( $\alpha$ ). Among various  $x_s$ 's and  $\alpha$ 's, the most effective sensing position

LINEAR PROPORTIONAL CONTROL OF SEPARATED FLOW

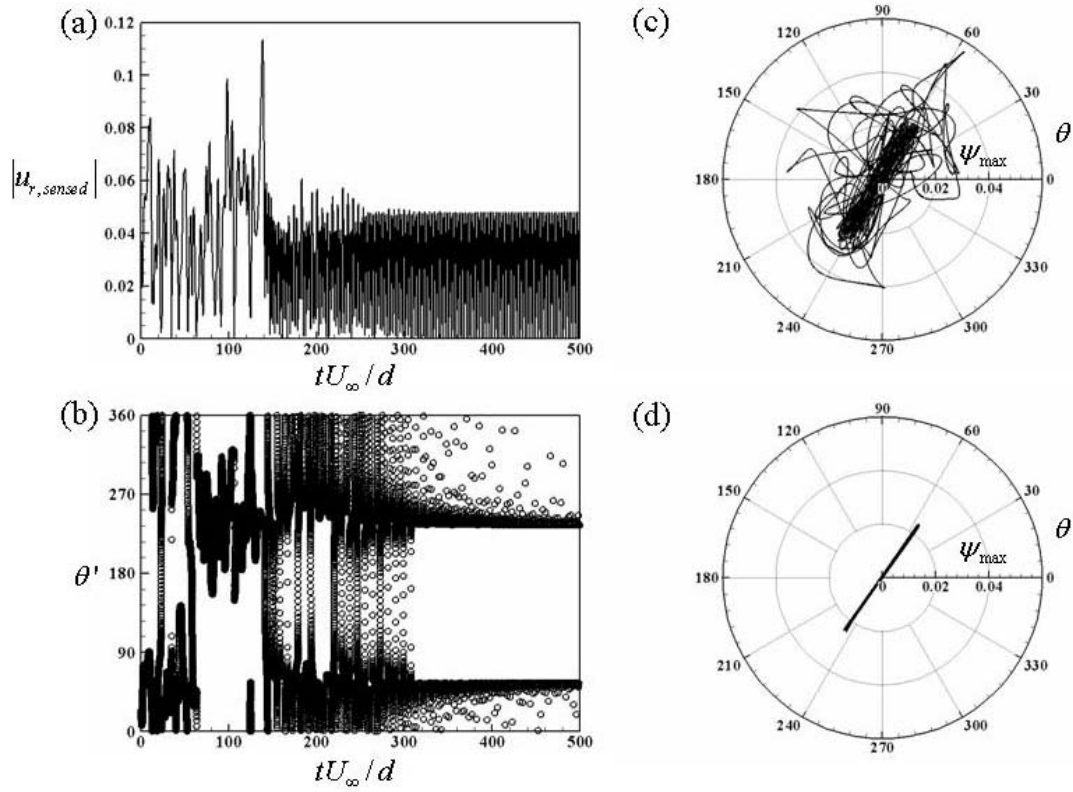


Figure 4. Time histories of the measured velocity and actuation velocity ( $x_s = 1.2d$  and  $\alpha = -0.5$ ;  $Re=425$ ): (a) magnitude of measured velocity; (b) azimuthal angle of measured velocity; (c) azimuthal angle and magnitude of maximum actuation for  $tU_{\infty}/d \leq 300$ ; (d) azimuthal angle and magnitude of maximum actuation for  $tU_{\infty}/d > 300$ .

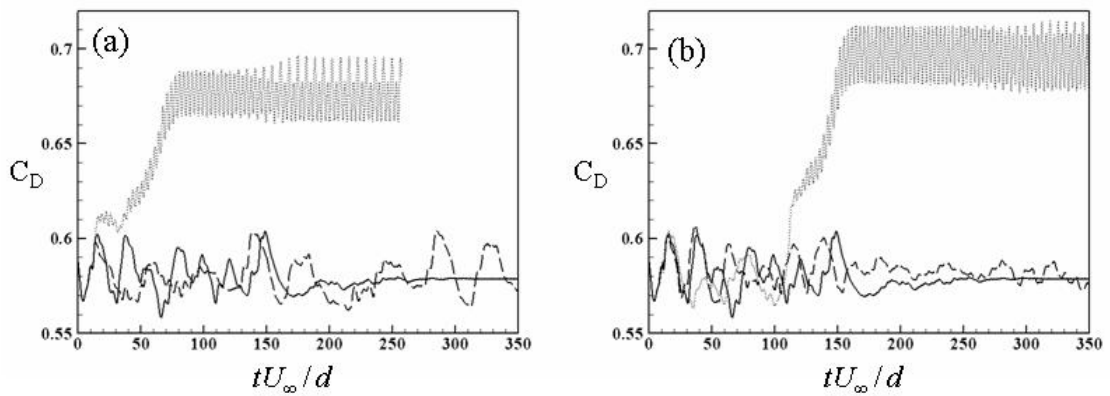


Figure 5. Variations of the drag coefficient with the sensing position and feedback gain ( $Re=425$ ): (a) ---,  $x_s/d = 1.1$ ; —, 1.2; ..., 1.3 ( $\alpha = -0.5$ ); (b) ---,  $\alpha = -0.4$ ; —, -0.5; ..., -0.6 ( $x_s = 1.2d$ ).

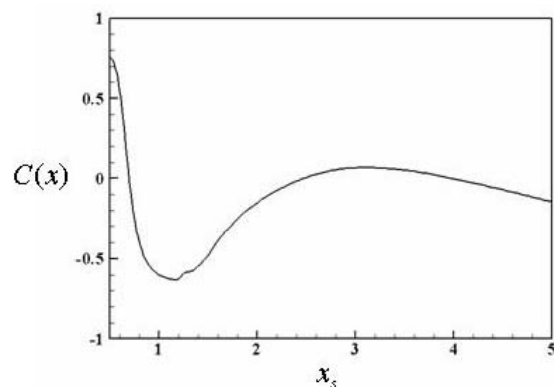


Figure 6. Correlation of the azimuthal angles between the lift and measured velocity (Re=425).

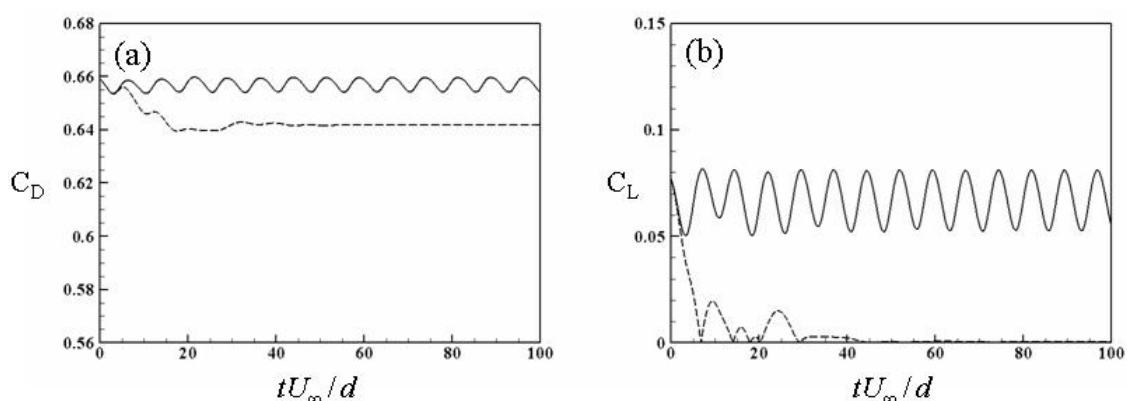


Figure 7. Time histories of the drag and lift coefficients (Re=300): —, without control; ---, with control. (a)  $C_D$ ; (b)  $C_L$ .

and amplitude are  $x_s = 1.2d$  and  $\alpha = -0.5$ , respectively. Figure 3 shows the time histories of drag and lift coefficients and the phase diagram at the final control state. Here, the lift coefficient is defined as  $C_L = \sqrt{C_y^2 + C_z^2}$ . The drag and lift fluctuations are significantly reduced by the control. However, the mean drag is almost unchanged. Figure 4 shows the variations of measured velocity and maximum actuation velocity. As shown in Figure 4, at the beginning of the control, the magnitude and azimuthal angle ( $\theta'$ ) of measured velocity vary significantly. At  $tU_\infty/d > 300$ ,  $\theta'$  is nearly fixed to be  $55^\circ$  and  $235^\circ$  (Figure 4 (b)). Therefore, the azimuthal angle of maximum actuation follows that of  $\theta'$  (Figure 4 (d)).

The present control method strongly depends on the feedback gain  $\alpha$  and sensing position  $x_s$ . As shown in Figure 5, when the sensing position or the feedback gain is changed slightly, the drag fluctuations do not decrease and even increase.

The fluctuations of lift coefficient are closely related with vortex shedding, and thus it is important to know the sensor location at which the radial velocity

along the centerline in the wake is connected with vortex shedding. For this purpose, we define a correlation function as follows:

$$C(x) = \frac{\int_0^T \cos(\theta_{C_L} - \theta_{u_r}) dt}{T}, \quad (4)$$

where  $\theta_{C_L}$  is the azimuthal angle of lift direction,  $\theta_{u_r}$  is the azimuthal angle of the direction of measured velocity at the sensing location and  $T$  is the time period of averaging. The value of  $C(x)$  becomes 1 when the directions of lift and measured velocity are equal to each other, and -1 when the directions are opposite. Thus, when  $|C(x)| \rightarrow 1$ , the lift force and measured velocity are well correlated. Figure 6 shows the variation of  $C(x)$  with  $x_s$ . One can observe a strong negative correlation at  $x_s = 1.2d$ . This result agrees well with the  $x_s$  location where the control performs well.

At  $Re=300$ , the fluctuations of drag and lift are also significantly reduced by the control (Figure 7). The feedback gain and the sensing position for successful results are  $\alpha=-1.0$  and  $x_s=1.2d$ , respectively.

## 5. Conclusion

The objective of the present study was to reduce the drag and lift fluctuations for flow over a sphere using a linear proportional control. The radial velocity at the centerline in the wake region was measured for the feedback and the control input was the blowing/suction at a part of the sphere surface. The azimuthal angle of maximum blowing was in phase or out of phase to the measured velocity according to the sign of feedback gain and amplitude of blowing/suction was proportional to the measured velocity. This linear proportional control was very sensitive to the sensing location. Using the present linear proportional control, the drag and lift fluctuations were significantly reduced for both  $Re=300$  and 425. It was found that the best sensing location for the present control is very well correlated with the radial velocity induced by the vortex shedding.

## Acknowledgements

The financial support from the National Research Laboratory Program through the Korean Ministry of Science and Technology is gratefully acknowledged.

## References

1. Achenbach, E., The effect of surface roughness and tunnel blockage on the flow past spheres. *J. Fluid Mech.*, **65** (1974) 113–125.

2. Akselvoll, K. and Moin, P. Large eddy simulation of turbulent confined coannular jets and turbulent flow over a backward facing step, *Report No. TF-63 (Thermoscience Division, Department of Mechanical Engineering, Stanford University)* (1995).
3. Bearman, P. W. and Harvey, J. K. Golf ball aerodynamics. *Aeronautical Quarterly* **May** (1976) 112-122.
4. Choi, H., Jeon, W.-P. and Kim, J. Control of flow over a bluff body. *Ann. Rev. Fluid Mech.* (2008), to appear.
5. Choi, J., Jeon, W.-P. and Choi, H. Mechanism of drag reduction by dimples on a sphere. *Phys. Fluids* **18** (2006) 014702.
6. Jeon, S., Choi, J., Jeon, W.-P., Choi, H. and Park, J. Active control of flow over a sphere at a sub-critical Reynolds number. *J. Fluid Mech.* **517** (2004) 113–129.
7. Johnson, Y. A. and Patel, V. C. Flow past a sphere up to a Reynolds number of 300. *J. Fluid Mech.* **378** (1999) 19–70.
8. Kim, H. J. and Durbin, P. A. Observations of the frequencies in a sphere wake and of drag increase by acoustic excitation. *Phys. Fluids* **31** (1988) 3260–3265.
9. Kim, J., Kim, D. and Choi, H. An immersed-boundary finite volume method for simulations of flow in complex geometries. *J. Comput. Phys.* **171(1)** (2001) 132–150.
10. Kim, J. and Moin, P. Application of a fractional-step method to incompressible Navier-Stokes equations. *J. Comput. Phys.* **59** (1985) 308.
11. Park, D. S., Ladd, D. M. and Hendricks E. W. Feedback control of von Karman vortex shedding behind a circular cylinder at low Reynolds numbers. *Phys. Fluids* **6** (1994) 2390–2405.
12. Suryanarayana, G. K., Pauer, H. and Meier, G. E. A. Bluff-body drag reduction by passive ventilation. *Exp. Fluids* **16** (1993) 73–81.